Received: 25.03.2018
Accepted: 05.04.2018

IMAGE PATTERN ANALYSIS WITH IMAGE POTENTIAL TRANSFORM

Oleg Butusov (ORCID: 0000-0003-1361-2121)
Faculty of Basic Competences
Moscow Polytechnic University, Moscow, Russia
e-mail: butusov-1@mail.ru
Vasily Dikusar
Russian Academy of Sciences, Moscow, Russia
e-mail: dikussar@yandex.ru

Abstract: Pattern analysis with image transform based on potential calculation was considered. Initial gray-scale image is sliced into equidistant levels and resulting binary image was prepared by joining of some levels to one binary image. Binary image was transformed under assumption that white pixels in it may be considered as electric charges or spins. Using this assumption Ising model and Coulomb model interaction between white pixels was used for image potential transform. The transform was calculated using moving window. The resulting gray-scale image was again transformed to binary image using the thresholding on 0.5 level. Further binary images were analyzed using statistical indices (average, standard deviation, skewness, kurtosis) and geometric signatures: area, eccentricity, Euler number, orientation and perimeter. It was found that the most suitable geometric signature for pattern configuration analysis of Ising potential transform (IPT) and Coulomb potential transform (CPT) is area value. Similarly the most suitable statistics is distance statistics between white pixels.

Keywords: binary image transform, distance and potential transform, statistical indices, geometric signatures, pattern analysis, pattern recognition

JEL classification: C52, C69

DOI: 10.22630/MIBE.2018.19.1.2

INTRODUCTION

Pattern analysis and recognition [1], data mining [2], classification [3] and clustering [4] are the most known problems in image processing. In some cases, image may show the multifractal properties and as a result fractal dimensions may be used as important characteristics of image patterns. So, fractal dimensions may be used for image classification or clustering. The advances in image fractal property study are widely used in different fields such as materials science [5], medicine [6-8], remote sensing [9,10] et al. Frequently objects on image are fuzzy and have fuzzy boundaries [11].

Different methods were developed for analysis of hidden pattern in images: stochastic methods and Markov random fields [12], morphological image processing [13], border detection [14], Fourier transform and wavelets [15,16], threshold or slicing binarization [17], texture analysis [18], genetic algorithms [19] et al. It should be noted that slicing binarization may be used to project complex structure of image into several pixel configurations which sometimes reflect peculiarities of inner patterns. In binarization the question of slicing levels is important. Several approaches may be used. Automatic thresholding was in details considered in [14]. The local adaptive thresholding was proposed by Bernsen [14]. For thresholding Bernsen used moving window and got threshold as average between maximum and minimum pixel values in the window. In [20] probabilities were used to find threshold between two pixels classes. Maximum entropy method is enough effective to calculate global threshold of gray-scale image [14, 21]. In case the histogram of gray-scale image has several modes the border between modes may be used as slicing measure.

After binarization binary images are often analyzed using mathematical morphology operations [22, 23] to discover hidden patterns. For example, in [23] binary image was received using water network mask. Further it was segmented using morphological calculation to three classes: core pixels, islet pixels and connector pixels.

A separate group of image processing algorithms comprise ones which are called distance transform (DT) algorithms [24]. There are many different methods and distance measures which are used in DT calculations. Euclidian distance DT (EDT) is the one of the popular distance measure for using in DT transform algorithms [25]. The problem of sparse object representation in discrete geometry was considered in [26]. The DT algorithm was also used in [27] for automatic pattern recognition. The problem of DT transform algorithm complexity was considered in [28]. It is well-known that EDT calculation is rather time-consuming operation. To solve this problem several effective algorithms were developed [28]: Linear-time Legendre transform (LLT) algorithm, the parabolic envelope (PE) algorithm and non-expansive proximal mapping (NEP) algorithm. It was shown in [28] that these algorithms have linear complexity and so may be effectively used for DT processing of binary images. Modern efficient means of parallel computing and computing with GPU are often used for EDT calculation [29]. DT proved to be useful in many practical applications. In medical imaging DT is one of best means for discovering the similarity between images. DT image transform is important for 3D study of inner organs using slice-by-slice method [30]. Good results were obtained using together watershed algorithm and DT for blood cell image segmentation [31]. Watershed algorithm needs grayscale images. So, DT transform may be used to transform binary image to gray-scale. In [31] watershed and distance transform algorithm were used together with four distances measures: EDT, city-block, chessboard and quasi-Euclidean. It was found in [31] that chess board DT measure has better results in watershed segmentation then Euclidean, city block and quasi-Euclidean DT measures [31].

In our present work we considered another three kinds of DT:

- Ising potential DT;
- Coulomb potential DT using white foreground pixels as positive charges;
- Coulomb potential DT using both white foreground pixels as positive charges and black background pixels as negative charges.

The proposed models of DT were used in present work for pattern recognition.

BINARIZATION

One of the popular method for detecting hidden patterns in image is simple binarization [20-23]. Sometimes binarization can produce good results after several successive binarizations of different kinds. Sometimes patterns show itself after using the union ('OR-operation') of several different binary slices. Let us call it nonlinear binarization.

Let us consider as working example the fragment (200x200 pixels) of microphotography of quartz glass (silicon dioxide). The original image and its histogram is shown in Figure1. To create binary image, one may use great variety of algorithms. One of the most simple algorithm is equal step quantization (ESQ) $\Delta b = (b_{\max} - b_{\min})/N$, where N – number of steps and N+1 – number of levels. Using ESQ one may take additional choices. It is possible to use for gray-scale image digitization the round, floor or ceil operations or their nonlinear variants. For example, one may use asymmetric rounding algorithm $k = \begin{cases} ceil(v), if\,(v - floor(v) \geq s) \\ floor(v),\ othervise \end{cases}$,where v – pixel value, s – threshold. Sometimes it is useful to join several binary slicing levels in one joined level (union with 'OR-operation'). This operation may be called '*nonlinear binarization*'. The operation may produce more complex patterns then simple slicing. Let us consider asymmetric binarization example in which original image (Figure 1) is splinted into 6-levels. The results are shown in Figure 2.

White points in Figure 2 are pixels containing ones ("one" or foreground-points) and black point are pixels – containing zeros ("zero" or background-points). Binary image is (0-1) matrix. Images in Figure 2 are the result of nonlinear binarization by joining (2,4,5)-slicing levels into one binary image.

Another one of the well-known binarization algorithms is the density algorithm. This algorithm is binary to binary transform algorithm and is based on using moving window (MW). Central pixel of MW is filled with ones if the density of white points inside moving window exceeds the specified threshold $t = \frac{n_b}{(2d+1)^2} \geq h$, where h – threshold, n_b – number of white pixels inside MW, d – half-width of moving window. In our calculation we used d = 3 or 5 pixels MW and h = 0.3 or 0.1. The size of resulting density image is (200-2d) x (200-2d) pixels. Figure 3 shows the result of Figure 2a density image transform.

DISTANCE TRANSFORM FOR PATTERN ANALYSIS

Distance transform algorithm is often used in none fuzzy object recognition as border detection means. This algorithm transforms a binary image to gray scale image (binary-to-gray scale algorithm). The foreground pixels in binary image are marked by "ones" (white points) and background pixels by "zero" (black points). DT-algorithm calculates distance from every foreground pixel to the nearest background pixel and assigns this value to the central pixel. Similarly, it calculates distance from background pixel to the nearest foreground pixel and assigns this value to the central pixel [24-31].

Figure 1. Original grayscale image and it histogram

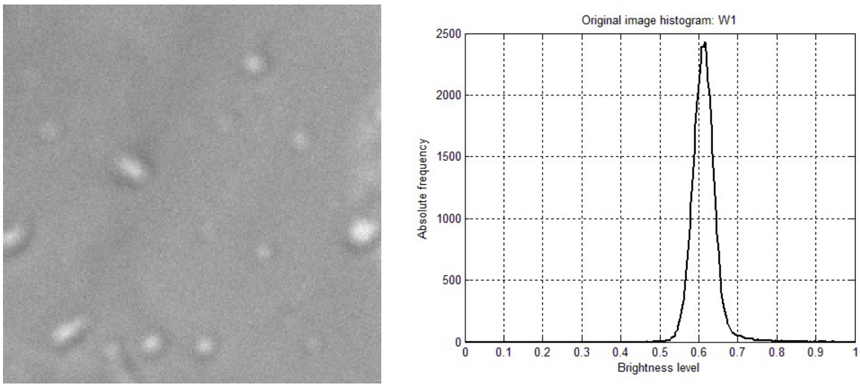

Source: own preparation

Figure 2. Asymmetric binarization of original image into 6-levels and joining up levels with numbers (2,4,5): (a) using threshold s = 0.2; (b) using threshold s = 0.4

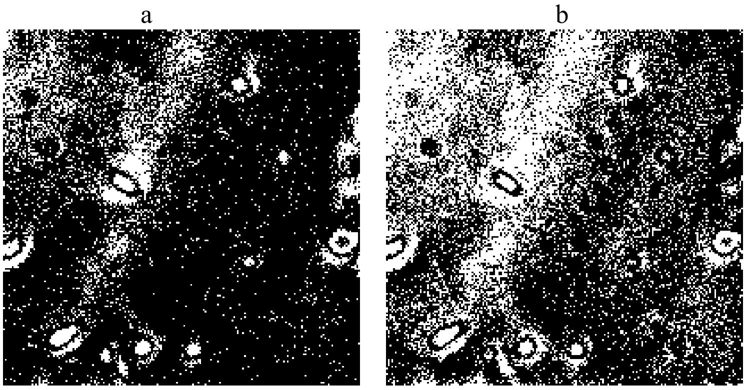

Source: own preparation

Figure 3. Binary images after density transform: (a) d = 3; h = 0.3; (b) d = 5; h = 0.3

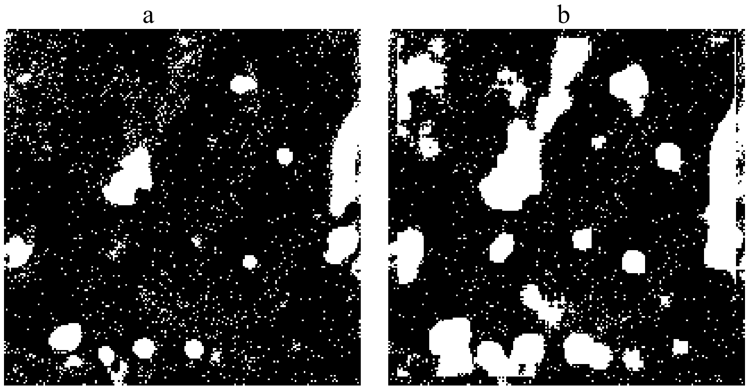

Source: own preparation

At present time some DT-algorithms were generalized to three and more dimensions. It is rather important for medical image processing as medical images often are three dimensional or consist of many two-dimensional slices of three dimensional organs [30].

DISTANCE TRANSFORM CALCULATION

In case of fuzzy foreground different forms of distance measures and distance transform may be used for hidden patterns analysis. For example, one may use moving window and calculate sum or average of all distances between white points in MW. The resulting value may be assigned to the central pixel. This algorithm may be called “moving window distance transform (MWDT)”. Let us consider distance measures used for MWDT transform of image in Figure 3a:

Squared Euclidian distance (SED):

$$SED(k,p)=\sum_G (i_1-i_2)^2+(j_1-j_2)^2 . \tag{1}$$

City-block distance (CBD):

$$CBD(k,p)=\sum_G |i_1-i_2|+|j_1-j_2| . \tag{2}$$

Chessboard distance (ChBD):

$$ChBD(k,p)=\sum_G \max(|i_1-i_2|,|j_1-j_2|). \tag{3}$$

Quasi-euclidean distance (QED):

$$QED(k,p)=\sum_G \begin{cases} |i_1-i_2|+(\sqrt{2}-1)|j_1-j_2|, if\ |i_1-i_2|>|j_1-j_2| \\ (\sqrt{2}-1)|i_1-i_2|+|j_1-j_2|, otherwise \end{cases} . \tag{4}$$

where: $G=b(i_1,j_1)=1, b(i_2,j_2)=1, (i_1,j_1)\in MW, (i_2,j_2)\in MW$; MW – moving window; (k,p) - coordinates of central pixel; $b(i,j)$ - pixel value.

The result of image from Figure 3a SED transform is shown in Figure 4. The transform was calculated using Intel Visual Fortran 2013 and Intel Parallel Studio XE [32]. The choice of programming language and Parallel Studio is due to high speed of computation and the possibility of vector-matrix calculations. The fragment of Fortran vectorized code is shown below:

```
real*4 :: s
integer*4 i, j, i1, j1, ii1, jj1
integer*4, dimension(:), allocatable:: b1, b2, rkp2
allocate(b1(b))
allocate(b2(b))
allocate(rkp2(b))
rkp2 = 0
s=0.0
do i=1,a
    b1 = Bw(i,:)
    do i1 = 1,a
        b2 = Bw(i1,:)
        ii1 = (i - i1)**2
        forall(j = 1:b, j1 = 1:b, b1(j) .eq. 1 .and. b2(j1) .eq. 1) rkp2(j) = ii1 + (j - j1)**2
        s = s + sum(rkp2)
    end do
end do
make_E=0.5*s
```

Figure 4. SED image transform: (a) normalized SED-image; (b) 0.5 level threshold binarization

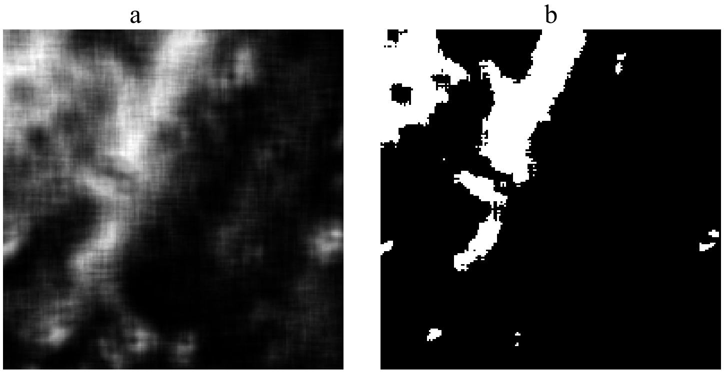

Source: own preparation

Additional patterns could be seen when compared Figure 2, Figure 3 and Figure 4. It should be noted that results of other metrics are visually indistinguishable from SED. Let us consider the histogram of difference between SED and CBD images (Figure 5). It shows that difference of pixel values is very small: $|SED - CBD| < 0.01$. So, to get additional hidden patterns one should use algorithms of other kind.

Figure 5. Histogram of image difference between SED and CBD metrics

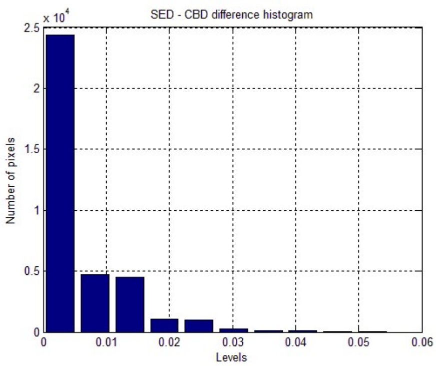

Source: own preparation

POTENTIAL TRANSFORM FOR PATTERN ANALYSIS

Let us assume that white points in binary image may be considered as particles. These particles create potential that may be calculated in the central pixel of MW. There are different kinds of particle interaction potential. There are distance dependent potentials (Coulomb potential) or distance independent potentials (Ising spin-spin interaction) [33] et al. In Ising model the spin-spin interaction is considered only between nearest spins [33]. In our study it corresponds to interaction only between particles in the limits of MW. In calculation we assume that white points have spin $S_i = 1$ and black points have spin $S_i = -1$. Also, we assume that total potential is the sum of two-particle interactions. So, we compute Ising potential as follows:

$$U_{I\sin g}(c) = -J \sum_{(t,q\in w)} S_t S_q = -\sum_{(t,q\in w)} (2b(t)-1)(2b(q)-1), \tag{5}$$

where: w – moving window; b – binary matrix of moving window; c – central point of moving window; t, q – white point numbers inside moving window; $S_t S_q \in \{1,-1\}$ – spin values of t-th and q-th white points; J – energy constant (in calculation used as $J = 1$).

In every position of MW, the total potential of spin interaction between particles is assigned to central pixel. The resulting gray-scale image we call Ising potential transform (IPT) of binary image.

In our study we also considered two algorithms with interaction of Coulomb type. The first algorithm (CPT1-algorithm) uses total potential of interaction only between white points (positive charge particles) $U(c) = \sum_{t<q} V(r_{t,q}) = \sum_{t<q} \frac{1}{r_{t,q}}$, where: $r_{t,q}$ - distance between two white points. We compute the total interaction between white particles as follows:

$$U(p,k) = \sum_G \frac{1}{\sqrt{(i_1 - i_2)^2 + (j_1 - j_2)^2}}, \tag{6}$$

where: w – moving window; (p,k) – central point of moving window; $G = \{t = (i_1, j_1) \neq q = (i_2, j_2) \neq c = (p,k) \in w, b(i_1, j_1) = 1, b(i_2, j_2) = 1\}$; b – binary image.

Second algorithm (CPT2-algorithm) uses for total potential calculation both white and black points (particles of any charge)

$$E(p,k) = \sum_G \frac{(2b(i_1, j_1) - 1)(2b(i_2, j_2) - 1)}{\sqrt{(i_1 - i_2)^2 + (j_1 - j_2)^2}}, \tag{7}$$

where $G = \{t = (i_1, j_1) \neq q(i_2, j_2) \neq c = (p,k) \in w\}$. The resulting gray-scale images we call Coulomb potential transform (CPT1 or CPT2) of binary image. We assume that using another kind of particle interaction, for example, the Lenard-Jones potential or Tersoff potential [34, 35], one may receive other patterns. Figure 6 shows resulting normalized gray-scale images of IPT, CPT1 and CPT2 for binary image in Figure 3a. Figure 7 shows their 0.5-threshold binarization and Figure 8 shows their histograms. From Figure 7a and Figure 7c it follows that resulting IPT and CPT2 show similar patterns.

Figure 6. Potential transforms of binary image from Figure 3a: (a) IPT; (b) CPT1-algorithm; (c) CPT2-algorithm

a b c

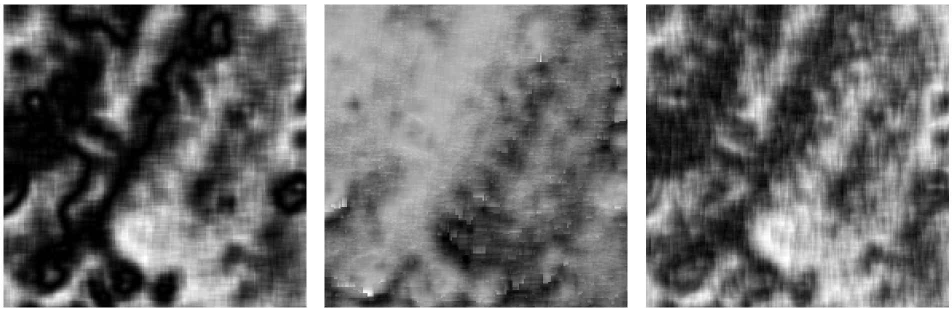

Source: own preparation

Figure 7. 0.5 level threshold binarization: (a) IPT; (b) CPT1-algorithm; (c) CPT2-algorithm

a b c

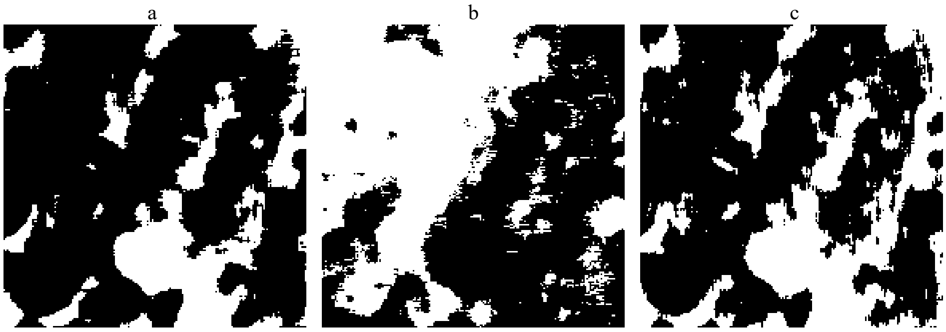

Source: own preparation

Figure 8. Histograms of potential transform gray-scale images: (a) IPT; (b) CPT1-algorithm; (c) CPT2-algorithm

a b c

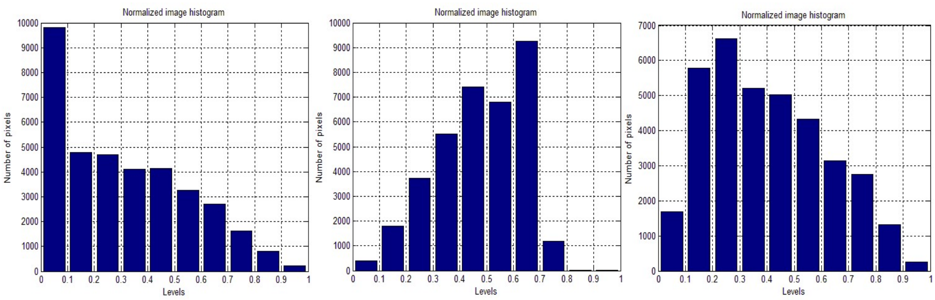

Source: own preparation

Histograms show pixel distribution in MWDT images. Binary images show patterns. The patterns differ by statistical and geometric properties. To study pattern we used several statistical and geometric characteristics. In statistical analysis we used the following normalized statistical indices:
Normalizes average:

$$\bar{x}^{(n)} = \frac{\frac{1}{N}\sum_{i=1}^{N} x_i}{\max_i(|x_i|)}, \tag{8}$$

Normalized standard deviation:

$$\sigma^{(n)} = \frac{\frac{1}{N-1}\sum_{i=1}^{N} (x_i - \bar{x})^2}{\max_i(|x_i - \bar{x}|)}, \tag{9}$$

Normalized skewness:

$$Sk^{(n)} = \frac{\frac{1}{N}\sum_{i=1}^{N} (x_i - \bar{x})^3}{\max_i(|x_i - \bar{x}|)^3}, \tag{10}$$

Normalized kurtosis:

$$Ku^{(n)} = \frac{\frac{1}{N}\sum_{i=1}^{N} (x_i - \bar{x})^4}{\max_i(|x_i - \bar{x}|)^4}. \tag{11}$$

In geometric analysis we used five signatures: area, eccentricity, Euler number, orientation and perimeter.
Area – it is total number of pixels which form pattern objects in binary image [15,36]. Area is calculated as follows:

$$N_k = \sum_{(i,j)\in\Omega_k} 1, \tag{12}$$

where: (i, j) - pixel; Ω_k - set of all pixels forming *k*-object.
Eccentricity – it is the eccentricity of the ellipse that has the same second-moments as the object [15, 36]. Eccentricity is calculated as follows:

$$\varepsilon = \frac{\sqrt{I_{\max}^2 - I_{\min}^2}}{I_{\max}}, \tag{13}$$

where: $I_{\max}, I_{\min}$ - are the lengths of maximum and minimum axis of inertia; $I_{\max} = 2\sqrt{2}\sqrt{U_x + U_y + D}$; $I_{\min} = 2\sqrt{2}\sqrt{U_x + U_y - D}$; $U_x = \frac{1}{12} + \sum_{(i,j)\in\Omega}(i - i_c)^2 \Big/ N_k$; $U_y = \frac{1}{12} + \sum_{(i,j)\in\Omega}(j - j_c)^2 \Big/ N_k$; $D = \sqrt{(U_x + U_y)^2 + 4U_{xy}^2}$; $U_{xy} = \frac{1}{N_k}\sum_{(i,j)\in\Omega}(i - i_c)(j - j_c)$
$i_c = \frac{1}{N_k}\sum_{(i,j)\in\Omega} i$; $j_c = \frac{1}{N_k}\sum_{(i,j)\in\Omega} j$.

Euler Number – it is the number of objects in the region minus the number of holes in these objects [15, 36].

Orientation – it is angle (in degrees ranging from -90 to 90 degrees) between the x-axis and the major axis of the ellipse that has the same second-moments as the binary image object. Orientation is calculated as follows:

$$R = \begin{cases} \frac{180}{\pi}\arctan\left(\frac{U_y - U_x + D}{2U_{xy}}\right), U_y > U_x \\ \frac{180}{\pi}\arctan\left(\frac{2U_{xy}}{U_y - U_x + D}\right), \textit{otherwise} \end{cases} . \tag{14}$$

Perimeter – is computed by calculating the distance between each adjoining pair of pixels around the border of the region [15, 36].

The result of statistical and geometric analysis is presented in Table 1. Statistics over all pixels in binary image denotes calculation of above indices for all both white and black pixels in binary image and statistics of distances between white pixels denotes the same calculation for the whole array of distances between white pixels.

Table 1. Normalized signatures of binary images of Figure 7

	Average	Standard deviation	Skewness	Kurtosis
IPT (Figure 7a)				
Object signatures				
Area	0.0458	0.1602	0.0222	0.0219
Eccentricity	0.5789	0.7388	-0.2260	0.4217
Euler Number	0.7083	0.1769	-0.0244	0.0230
Orientation	0.1327	0.4262	-0.0174	0.1066
Perimeter	0.0832	0.2017	0.0295	0.0271
Statistics over all pixels of binary image				
	0.2375	0.5581	0.2145	0.2447
Statistics of distances between white pixels				
	0.1631	0.1918	0.0087	0.0034

Table 1. continued

	Average	Standard deviation	Skewness	Kurtosis
CPT1 (Figure 7b)				
Object signatures				
Area	0.0089	0.0899	0.0080	0.0081
Eccentricity	0.5230	0.8025	-0.1820	0.5279
Euler Number	0.3810	0.0903	-0.0080	0.0081
Orientation	0.0928	0.3180	0.0343	0.0544
Perimeter	0.0149	0.0913	0.0080	0.0081
Statistics over all pixels of binary image				
	0.4784	0.9576	0.0761	0.8473
Statistics of distances between white pixels				
	0.1411	0.1603	0.0004	0.0007
CPT2 (Figure 7c)				
Object signatures				
Area	0.0210	0.1210	0.0142	0.0143
Eccentricity	0.4807	0.8281	-0.0964	0.5355
Euler Number	0.6528	0.1208	-0.0142	0.0143
Orientation	0.0969	0.4929	-0.0056	0.1581
Perimeter	0.0299	0.1243	0.0142	0.0143
Statistics over all pixels of binary image				
	0.3265	0.6962	0.2498	0.3636
Statistics of distances between white pixels				
	0.1648	0.1846	0.0047	0.0018

Source: own calculations

It follows from Figure 7a and Figure 7c that patterns in them are similar. So, we may use values in Table 1 as criteria for assessment of different statistical and geometric characteristics efficiency. The according graphs are shown in Figure 8.

Figure 9. Signature graphs: (a) – Average; (b) – Standard deviation; (c) – Skewness; (d) Kurtosis; symbols on x-axis denote: ‘A’ – Area, ‘E’ – Eccentricity, ‘EN’ – Euler Number, ‘Or’ – Orientation, ‘P’ – Perimeter, ‘S’ - statistics over all pixels of binary image, ‘RR’ - statistics of distances between white pixels; solid line – IPT; dotted line – CPT2

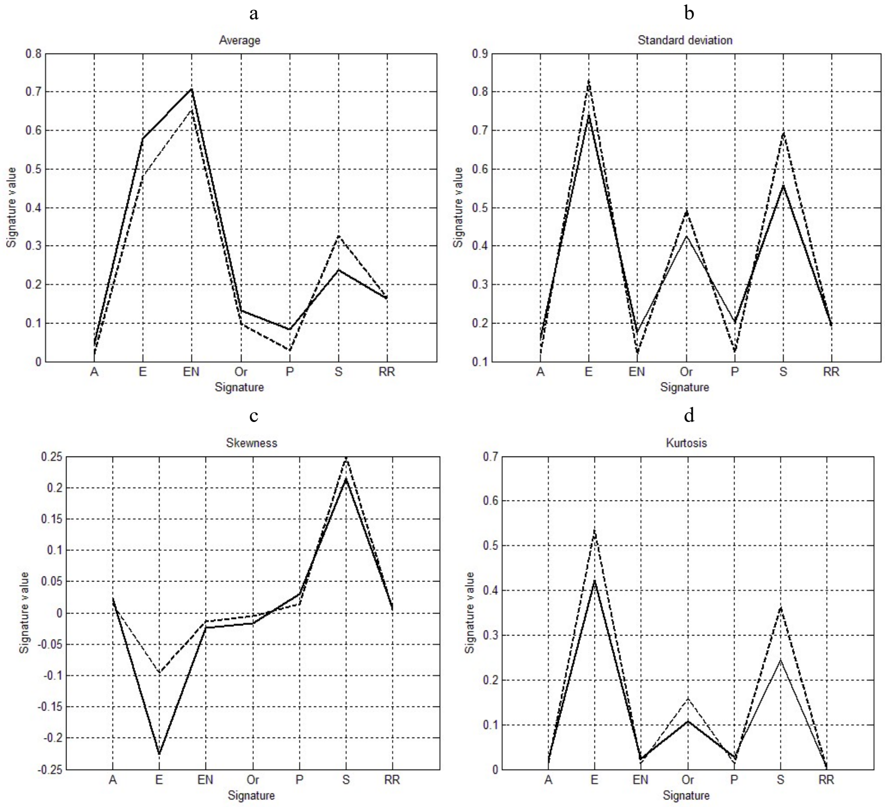

Source: own preparation

Figure 9 disclose the following satisfactory quantitative similarity between statistical - geometric combinations: (1) ‘Area - Average’; (2) ‘Distances between white pixels - Average’; (3) ‘Area – Standard deviation’; (4) ‘Distances between white pixels - Standard deviation’; (5) ‘Area - Skewness’; (6) ‘Euler Number - Skewness’; (7) ‘Orientation - Skewness’; (8) ‘Perimeter - Skewness’; (9) ‘Distances between white pixels - Skewness’; (10) – ‘Area - Kurtosis’; (11) ‘Euler Number - Kurtosis’; (12) ‘Perimeter - Kurtosis’; (13) ‘Distances between white pixels - Kurtosis’. Most often in combinations occur: ‘Area’ and ‘Distances statistics between white pixels’. So, these signatures may be proposed as satisfactory quantitative similarity criteria in comparing patterns in binary image.

CONCLUSION

At the present time image pattern analysis and recognition is of great practical interest for different applications. For example, the discovering of hidden patterns in image is of great importance for image biology, image medicine, material sciences et al. Many methods were worked out for pattern analysis including distance image transform. In this study we propose the potential transform as additional means for discovering hidden patterns in binary image. Three potentials were proposed:

- Ising model potential;
- Coulomb potential only from a system of positive charges (white foreground pixels) – CPT1-algorithm;
- Coulomb potential of a system both of positive (white foreground pixels) and negative charges (black background pixels) – CPT2-algorithm.

All calculations were made using moving window of a square shape with five pixels half-width. The resulting gray-scale images were transformed to binary images, using 0.5 thresholding.

Patterns in binary images were analysis using following statistical indices: average, standard deviation, skewness and kurtosis. Also we used the following geometric signatures: area, eccentricity, Euler number, orientation, perimeter. Statistical indices were also calculated for white - black pixel arrangement and for distance statistic between white pixels.

It was found that the most suitable geometric signature for pattern configuration analysis of IPT and CPT is area value. Similarly the most suitable statistics is distance statistics between white pixels.

REFERENCES

1. Cornelius T. Leondes (eds) (1998) Image Processing and Pattern Recognition. Academic Press.
2. Santosh Kumar Dash, Mrutyunjaya Panda (2016) Image Classification using Data Mining Techniques. Advances in Computer Science and Information Technology (ACSIT), 3(3) 157-162.
3. Arunadevi S., Daniel Madan Raja S. (2014) A Survey on Image Classification Algorithm Based on Per-pixel. International Journal of Engineering Research and General Science, 2(6), 387-392.
4. Fu K. S., Mui J. K. (1981) A Survey on Image Segmentation. Pattern Recognition, 13, 3-16.
5. Amanpreet Kaur (2014) A Review Paper on Material Analysis using Image Processing. International Journal of Science and Research (IJSR), 3(10), 624-625.
6. Reljin I. S., Reljin B. D. (2002) Fractal Geometry and Multifractals in Analyzing and Processing Medical Data and Images. Archive of Oncology, 10(4), 283-293.

7. Lopes R., Betrouni N. (2009) Fractal and Multifractal Analysis: a Review. Medical Image Analysis, 13(4) 634-649.
8. Uahabi K. L., Atounti M. (2015) Applications of Fractals in Medicine. Annals of the University of Craiova, Mathematics and Computer Science Series, 42(1), 167-174.
9. Image Processing for Remote Sensing (2006) CRC Press, Taylor & Francis Group.
10. Chen C.H. (2008) Image Processing for Remote Sensing. United States of America, Taylor & Francis Group, LLC.
11. James C. Bezdek, James Keller, Raghu Krisnapuram, Nikhil R. Pal (2005) Fuzzy Models and Algorithms for Pattern Recognition and Image Processing. Springer Science+Business Media, Inc.
12. Chee Sun Won, Robert M. Gray (2004) Stochastic Image Processing. Springer Science+Business Media New York.
13. Edward R. Dougherty, Roberto A. Lotufo (2003) Hands-on Morphological Image Processing. SPIE, Bellingham, Washington.
14. Wilhelm Burger, Mark J. Burge (2013) Principles of Digital Image Processing. Advanced Methods, Springer-Verlag London.
15. Rafael C. Gonzalez, Richard E. Woods (2008) Digital Image Processing. Pearson Education, Inc.
16. S. Allen Broughton, Kurt Bryan (2009) Discrete Fourier Analysis and Wavelets. John Wiley.
17. Stephane Marchand-Maillet, Yazid M. Sharaiha (2000) Binary Digital Image Processing. Academic Press.
18. Maria Petrou, Pedro Garcia Cevilla (2006) Image Processing. Dealing with Texture. John Wiley.
19. Stefano Cagnoni, Evelyne Lutton, and Gustavo Olague (eds) (2007) Genetic and Evolutionary Computation for Image Processing and Analysis. Hindawi Publishing Corporation.
20. P.-S. Liao, T.-S. Chen, and P.-C. Chung (2001) A Fast Algorithm for Multilevel Thresholding. Journal of Information Science and Engineering, 17, 713-727.
21. J. N. Kapur, P. K. Sahoo, and A. K. C. Wong (1985) A New Method for Gray-level Picture Thresholding using the Entropy of the Histogram. Computer Vision, Graphics, and Image Processing, 29, 273-285.
22. Frank Y. Shih (2009) Image Processing and Mathematical Morphology. Fundamentals and Applications. CRC Press, Taylor & Francis Group.
23. Pierre Soille, Peter Vogt (2009) Morphological Segmentation of Binary Patterns. Pattern Recognition Letters, 30, 456-459.
24. Borgefors G. (1986) Distance Transform in Digital Image. Computer Vision, Graphics and Image Processing, 34, 344-371.
25. Danielsson P-E. (1980) Euclidean Distance Mapping. Computer Graphics Image Processing, 14, 227-248.
26. Strand R. (2011) Sparse Object Representations by Digital Distance Functions. Discrete Geometry for Computer Imagery, 6607 in Lecture Notes in Computer Science. Springer Berlin Heidelberg, 211-222.
27. Abdul Ghafoor, Rao Naveed Iqbal, and Shoab Khan (2003) Image Matching using Distance Transform. Image Analysis, 13th Scandinavian Conference, SCIA Halmstad,

Sweden, June 29 - July 2, 2003, Proceedings. Springer-Verlag Berlin Heidelberg, 654-660.

28. Yves Lucet (2009) New Sequential Exact Euclidean Distance Transform Algorithms based on Convex Analysis. Image and Vision Computing, 27, 37-44.
29. Cuntz N., Kolb A. (2007) Fast Hierarchical 3D Distance Transforms on the GPU. Eurographics, 93-96.
30. Eşref Selvi, Merve Özdemir and M. Alper Selver (2013) Performance Analysis of Distance Transform based Inter-slice Similarity Information on Segmentation of Medical Image Series. Mathematical and Computational Applications, 18(3), 511-520.
31. CH. Nooka Raju, G. S. N. Raju, V. K. Varma Gottumukkala (2016) Studies on Watershed Segmentation for Blood Cell Images using Different Distance Transforms. IOSR Journal of VLSI and Signal Processing (IOSR-JVSP), 6(2), 79-85.
32. Intel Parrallel studio-xe, https://software.intel.com/en-us/parallel-studio-xe.
33. Binder K., Heermann D. (2010) Monte Carlo Simulation in Statistical Physics. 5th Ed. Springer.
34. Rapaport D. C. (1995) The Art of Molecular Dynamics Simulation. Cambridge, New York, Cambridge University Press.
35. Tersoff J. (1989) Modeling Solid-state Chemistry: Interatomic Potentials for Multi-component Systems. Physical Review B, 39, 5566-5568.
36. Matlab help system. https://www.mathworks.com/.